IEEE Trans. Nucl Sci., vol. NS-45, pp. 462–466, 1998

Prospects for Dense, Infrared Emitting Scintillators*

W. W. Moses, M. J. Weber, S. E. Derenzo, D. Perry, P. Berdahl, and L. A. Boatner‡
Lawrence Berkeley National Laboratory, University of California, Berkeley, CA 94720 USA
‡Oak Ridge National Laboratory, Oak Ridge, TN 37831 USA

Abstract

We present results from an ongoing search for inorganic scintillators for x- and gamma- ray detection. We measure the scintillation properties (luminous efficiency, decay time, and emission wavelength) of powdered samples excited by brief x-ray pulses. To find scintillators that are compatible with silicon photodetectors, we have tested over 1,100 samples using a photomultiplier tube with a GaAs:Cs photocathode, which is sensitive to 200–950 nm emissions. Optical filters are used to block emissions that are observable with bialkali PMTs. Several lanthanide and transition metal ions, molecular complexes, and II-VI compounds are known to have strong emissions at wavelengths >500 nm. We find that several compounds exhibit emission intensities comparable to commercial phosphors in the 600–900 nm range, including Eu and Sm doped $LuPO_4$, $ScPO_4$, and YPO_4. Significant emissions are also observed from Tb, Dy, Er, Pr, and Tm doped phosphates, as well as several intrinsic compounds, notably Hg_2Cl_2. Scintillation characteristics of promising compounds (in powdered or small crystal form) are presented.

I. Introduction

We have previously described [1, 2] a method for finding new scintillators by measuring the scintillation properties (luminous efficiency, decay time, and emission wavelength) of powdered samples excited with brief x-ray pulses [3-5]. By synthesizing and testing candidate compounds as powders, the difficult task of obtaining large, optically clear samples is only performed for the most promising compounds. Over 1,100 powdered samples have been measured, including both intrinsic and doped compounds. This search method has yielded several candidate materials, including cerium fluoride [6], lead tungstate [1], $LuAlO_3$:Ce [7], and the materials described herein. We are extending this search to cover longer emission wavelengths, since applications utilizing silicon photodiodes as optical detectors would benefit from scintillators that emit in the 550–1050 nm wavelength region. Many potentially useful materials may have been overlooked in previous searches which used bialkali photomultiplier tubes (PMTs) that are insensitive to emissions in this wavelength range. Longer wavelength scintillators would also be useful in applications requiring transmission through long optical fibers because of the lower fiber losses at longer wavelengths [8].

II. Methods

Powdered samples are measured by exciting them with 20 to 30 keV, 1 μs wide x-ray pulses from the table top pulsed x-ray unit shown in Figure 1 and observing their emission intensity with a red- and near infrared sensitive PMT. The x-ray tube is identical to one described earlier [4] , but with a pulsed (1 μs square wave) blue LED as an excitation source rather than a laser diode. This increases the number of x-rays per pulse from 4 sr^{-1} to 2,500 sr^{-1} at the expense of a significantly longer pulse width.

Each sample is placed in a quartz cuvette (50 mm long, 5.0 mm outer diameter, 0.37 mm wall thickness). The cuvette is placed in a light-tight box and excited by the 20-30 keV x-ray beam. Some fluorescent photons from the sample reach a PMT whose output is measured. Comparison of the PMT output rate to that with powdered BGO scintillator (assumed to have a luminosity of 8,200 photons/MeV [9]) is then used to estimate the emission intensity. Some samples have individual grains that are not powders (~1 μm typical dimension), but are small (0.5 mm typical dimension) crystals. This reduces their optical attenuation (as compared to a powder) and so artificially increases their measured luminosity, typically by a factor of 2–5 [2]. By recording the time difference between the end of the 1 μs long x-ray pulse and the scintillation signal with the delayed coincidence method [10], the fluorescent lifetime is measured. By inserting a computer controlled scanning monochromator between the sample and the PMT, the emission spectrum is measured [5]. This spectrum is corrected for the wavelength dependent efficiency of the monochromator, but not of the PMT.

To be sensitive to emissions with >500 nm wavelength, we use a Hamamatsu R 943-02 PMT with a GaAs:Cs photocathode, which has high sensitivity to emissions from 200–900 nm and has a relatively flat response (70 mA/W) between 300 and 850 nm (Figure 2). The quantum efficiency and dark current (when cooled to –20° C) of this PMT are comparable to a bialkali PMT at room temperature. Because of the electron optics of this design (a “side-on” PMT in an “end-on” package), the single photoelectron transit time jitter is ~4 ns fwhm. To restrict our sensitivity to the 600–900 nm range, a pair of filters (Hoya O-54 and R-62) are placed in the optical

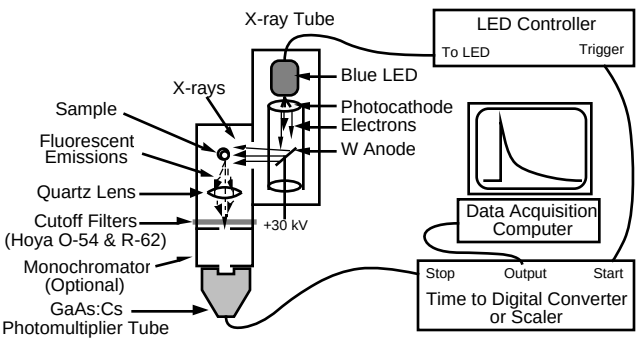

Figure 1. Measurement Apparatus. X-rays from the pulsed x-ray tube impinge on a powdered sample in a quartz cuvette, and the resulting fluorescent emissions are detected by a PMT. The counting rate measures fluorescent intensity, the delayed coincidence method is used to measure the fluorescent decay time, and the emission spectrum is measured by inserting a monochromator into the optical path.

* This work was supported in part by the U.S. Department of Energy under Contract No. DE-AC03-76SF00098, and in part by Public Health Service Grant No. P01-CA48002 from the National Cancer Institute of the National Institutes of Health.

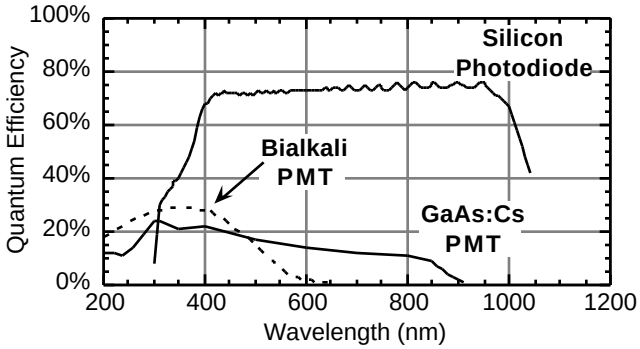

Figure 2. Typical quantum efficiency versus wavelength for various photodetectors.

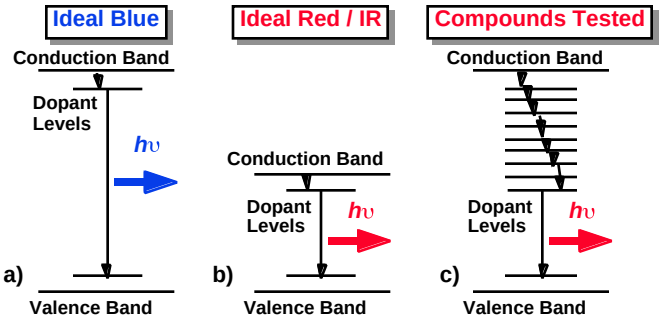

Figure 3. Energy level diagram of (a) an ideal blue emitting scintillator, (b) an ideal red emitting scintillator, and (c) the compounds tested in this work.

path. A pair (rather than a single filter) is used to reduce filter fluorescence [11], and the filters are kept in the dark for a day before data collection to minimize phosphorescence.

III. Sample Selection

A simplified band structure diagram for a classical "blue" emitting scintillator is shown in Figure 3a. Ionizing radiation promotes electrons from the valence band to the conduction band, with the number of electron / hole pairs being roughly equal to the deposited energy divided by three times the band gap energy. The electron and hole are transferred non-radiatively to an activating dopant whose ground and excited state energy levels lie within the band gap of the host material. This puts the dopant into an excited state from which it relaxes by producing a scintillation photon. An example of this type of material is NaI:Tl. The ideal red or infrared scintillator (Figure 3b) would have the same general characteristics, but the band gap energy of the host material would be significantly less (roughly half) than that of a blue scintillator and the energy levels of the activating dopant would be correspondingly closer together. This would yield a maximum possible scintillation efficiency that is roughly twice that of a blue scintillator because the smaller band gap energy yields a correspondingly higher number of electron / hole pairs.

Most of the samples used in this study are large band gap materials since they were initially selected as candidates for blue scintillators. Therefore, those samples studied here that exhibit red or infrared scintillation are most likely described by Figure 3c. The band gap for the host is the same as for the blue scintillator in Figure 3a, while the energy level difference between the activator excited and terminal states (which determines the wavelength of emitted photons) is the same as for the infrared scintillator in Figure 3b. Efficient transfer of the electron from the conduction band to the activator excited state is possible through multiple non-radiative transitions through intermediate energy levels, which are common in rare earth ions having more than one optically active electron.

Solid-state laser material research has shown that many of the rare earth elements (notably Pr^{3+}, Nd^{3+}, Sm^{3+}, Eu^{3+}, Eu^{2+}, Tb^{3+}, Ho^{3+}, Er^{3+}, Tm^{3+}, and Yb^{3+}) and several other ions (notably Cr^{3+} and Ti^{3+}) have intense room temperature emissions when incorporated as dopants into a variety of hosts [12]. Table 1 lists luminescent transitions in rare earth ions that have been used to demonstrate laser action in the 540 – 1100 nm region. While most have decay lifetimes of hundreds of microseconds to many milliseconds, there are some (*e.g.* Eu^{2+}, Ce^{3+}, Fe^{3+}, Ti^{3+}) with decay times of a few microseconds or less. Note that the wavelengths are only approximate; the exact wavelengths and fluorescence lifetimes depend on the host material, the specific Stark levels, and the temperature.

IV. Luminosity Measurements

We tested >1,100 compounds for 600–900 nm scintillation and observed intensities comparable to commercial phosphors for Eu and Sm doped $LuPO_4$, $ScPO_4$, and YPO_4. Significant emissions are also observed in Tb, Dy, Er, Pr, and Tm doped phosphates and several intrinsic compounds. Table 2 lists the luminous intensities of compounds with light output (in the 600–900 nm range) ≥900 photons/MeV. Data for all compounds is available in the red_luminosity.dat file via anonymous FTP to scint.lbl.gov [13].

V. Decay Lifetime Measurements

The decay time distributions were measured and fit with a sum of exponential components plus a constant term for the 100 most luminous compounds (corresponding to all compounds with luminosity >15% that of BGO). The pulse repetition rate was 1 kHz, so components longer than ten times the period (*i.e.* 10 ms) are included in the "constant" term. The most luminous compounds (generally europium and samarium doped materials) all were fit well by a single exponential component with >100 µs decay time. Figure 4 shows the luminous intensity versus the decay time of the europium doped compounds, as well as the host matrix and dopant concentration. Two of the compounds (Y_2O_3:Eu and

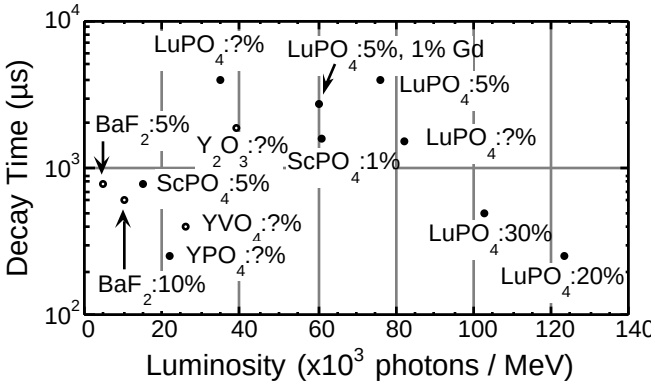

Figure 4. Luminous intensity versus decay lifetime for europium doped compounds. Compounds whose physical form is small crystals are shown with solid circles; powdered compounds are shown as open circles.

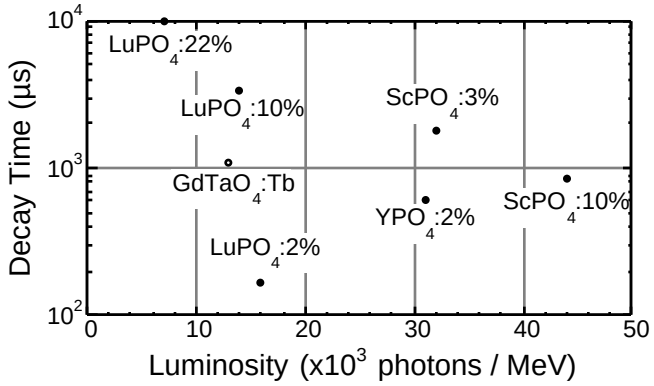

Figure 5. Luminous intensity versus decay lifetime for samarium doped compounds and one terbium doped compound. Small crystals are shown with solid circles; powdered compounds are shown as open circles.

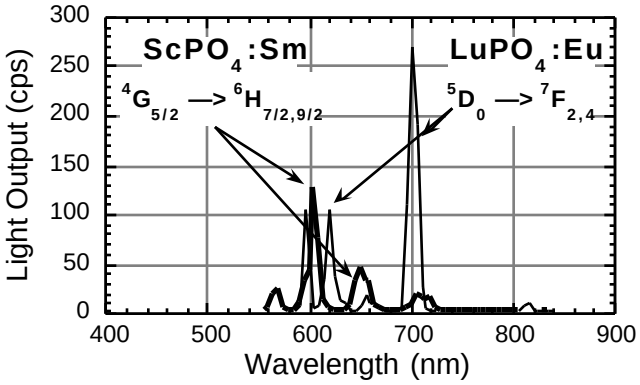

Figure 6. Emission spectra (corrected for wavelength dependence of monochromator efficiency, but not for PMT dependence) for representative europium and samarium doped samples.

YVO_4:Eu) are commercial phosphors. Figure 5 is a similar plot for samarium (and one terbium) doped compounds.

Finally, scintillators with both high luminosities and short decay times were searched for by identifying compounds with ≥3000 photons / MeV luminosity, more than 25% of the light emitted with a decay time ≤15 µs, and no significant long (>100 µs) component. The compounds identified by these selection criteria are listed in Table 3.

VI. Emission Spectra

The red and infrared emission wavelengths of most rare earth ions usually depend only weakly on the host material, as they do not involve transitions with the outermost orbitals and thus the relevant orbitals are shielded from the crystal field. The compounds in Figures 4 and 5 are no exception, so the emission spectra of the europium doped samples differ significantly from each other only in intensity, and the samarium doped samples are similarly self consistent. Figure 6 shows a representative spectrum for each dopant.

VII. Material Properties

Scintillators for x-ray and gamma ray detection should, in general, have high density and atomic number in order to provide high detection efficiency in small volumes. The density, attenuation length, and photoelectric fraction (at 511 keV) for all compounds included in Figure 4, Figure 5, and Table 3 are shown in Table 4. Of these compounds, only $LuPO_4$, BaF_2, $GdTaO_4$, Hg_2Cl_2, and SrI_2 have attenuation lengths ≤2.5 cm and photoelectric fractions ≥10%.

Table 3. Compounds with Fast Decay Components. Compounds with luminosity >3,000 photons / MeV and >25% of the light emitted with <15 µs decay time.

Compound	Luminosity (photons / MeV)	Decay Lifetime
Hg_2Cl_2	7,900	22% @ 3.0 µs 58% @ 13 µs 20% @ 21 µs
$ScPO_4$:1.7% Nd	6,700	30% @ 3.2 µs 70% @ 80 µs
TiO_2	4,400	380 ns
$BaSbNb_4O_{12}$	4,300	2.3 µs
SrI_2	3,800	560 ns
$SrTiO_3$	3,200	630 ns

VIII. Discussion

Prospects for red and infrared emitting scintillators with properties significantly better than those identified here are excellent, since few of the compounds investigated herein include host materials with the narrow (2–3 eV) band gap that is most likely to lead to efficient scintillation. As noted earlier, this investigation dealt with a collection of materials specifically of interest for their possible blue-near UV emission. There are, however, many materials that luminesce in the red and near-infrared that are not included here, several of which warrant study as potential red-infrared scintillators. One group are the smaller band gap semiconductor materials. The

Table 4. Material Properties of Compounds. The density, attenuation length, and photoelectric fraction (at 511 keV) for the samples in Figures 4 and 5 and Table 3.

Compound	Density (g / cm^3)	Attenuation Length (cm)	Photoelectric Fraction
$LuPO_4$	6.53	1.4	30%
$ScPO_4$	3.71	3.2	0.4%
YPO_4	4.28	2.8	4.0%
YVO_4	4.23	2.9	4.0%
BaF_2	4.89	2.3	19%
Y_2O_3	5.01	2.4	6.6%
$GdTaO_4$	8.84	1.0	34%
Hg_2Cl_2	7.2	1.1	46%
TiO_2	4.26	2.8	0.7%
$BaSbNb_4O_{12}$	?	?	9.9%
SrI_2	4.55	2.5	18%
$SrTiO_3$	5.12	2.4	4.0%

red scintillation properties of tellurium-doped CdS (density 4.82 g/cm^3) and ZnTe (6.2 g/cm^3) have been reported and compared with those of CsI(Tl) and $CdWO_4$ [14]. Other II-VI compounds of comparable density and with known emission in the near infrared include ZnSe (5.4 g/cm^3) and CdTe (6.2 g/cm^3). Among the III-V compounds GaAs (5.3 g/cm^3) and InP (4.8 g/cm^3) are known emitters in the near infrared.

While most Ce^{3+} activated scintillators emit in the near-UV and blue, green (SrS – 3.7 g/cm^3 [15]) and red (CaS – 2.5 g/cm^3 [16], Lu_2S_3 – 6.25 g/cm^3 [17], Y_2O_2S – 6.2 g/cm^3 [18], Lu_2O_2S – ~8.8 g/cm^3 [18]) emitters have been reported. Of the iron transition group ions, the Fe-doped phosphates reported here and Ti^{3+}-doped $YAlO_3$ [19] warrant further characterization.

IX. Conclusion

Over 1,100 compounds have been examined for emissions in the 600–900 nm range, which are appropriate for readout with silicon photodiodes. The most luminous compounds are Eu and Sm doped $LuPO_4$, $ScPO_4$, and YPO_4, which possess emission intensities comparable to that of commercial phosphors. However, none of these compounds have a major scintillation decay component of 100 μs or less and only $LuPO_4$ has a reasonably high photoelectric fraction and short attenuation length. $GdTaO_4$:Tb has a luminosity roughly 50% higher than BGO, high photoelectric fraction, and short attenuation length, but has an emission lifetime of nearly 1 ms. Undoped Hg_2Cl_2 [20] emits at 720 nm, has a luminosity and density comparable to that of BGO, and exhibits a reasonably fast non-exponential decay lifetime (5–25 μs decay constant).

X. Acknowledgment

We would like to thank Dr. N. B. Singh of Northrup-Grumman for preparation of the mercurous halide samples. This work was supported in part by the Director, Office of Energy Research, Office of Biological and Environmental Research, Medical Applications and Biophysical Research Division of the U.S. Department of Energy under contract No. DE-AC03-76SF00098 and in part by the National Institutes of Health, National Cancer Institute under grant No. R01-CA48002. Reference to a company or product name does not imply approval or recommendation by the University of California or the U.S. Department of Energy to the exclusion of others that may be suitable.

XI. References

[1] S. E. Derenzo, W. W. Moses, J. L. Cahoon, et al., "Prospects for new inorganic scintillators," *IEEE Trans. Nucl. Sci.*, vol. NS-37, pp. 203-208, 1990.

[2] S. E. Derenzo, W. W. Moses, J. L. Cahoon, et al. X-ray fluorescence measurements of 412 inorganic compounds. Proceedings of The IEEE Nuclear Science Symposium, pp. 143-147, (Edited by G. T. Baldwin), Santa Fe, NM, 1991.

[3] S. E. Derenzo, W. W. Moses, S. C. Blankespoor, et al., "Design of a pulsed x-ray system for fluorescent lifetime measurements with a timing resolution of 109 ps," *IEEE Trans. Nucl. Sci.*, vol. NS-41, pp. 629–631, 1994.

[4] S. C. Blankespoor, S. E. Derenzo, W. W. Moses, et al., "Characterization of a pulsed x-ray source for fluorescent lifetime measurements," *IEEE Trans. Nucl. Sci.*, vol. NS–41, pp. 698–702, 1994.

[5] W. W. Moses, S. E. Derenzo, M. J. Weber, et al., "Scintillator characterization using the LBL pulsed x-ray facility," *Rad. Meas.*, vol. 24, pp. 337–341, 1995.

[6] W. W. Moses and S. E. Derenzo, "Cerium fluoride, a new, heavy fast scintillator," *IEEE Trans. Nucl. Sci.*, vol. NS-36, pp. 173-176, 1989.

[7] W. W. Moses, S. E. Derenzo, A. Fyodorov, et al., "$LuAlO_3$:Ce – a high density, high speed scintillator for gamma detection," *IEEE Trans. Nucl. Sci.*, vol. NS-42, pp. 275–279, 1995.

[8] H. Takahashi, D. Fukuda, F. Jensen, et al., "The use of 1.5 μm infrared light from a cooled scintillator for optical fiber based system," *IEEE Trans. Nucl. Sci.*, vol. NS-43, pp. 1321–1323, 1996.

[9] I. Holl, E. Lorenz, and G. Mageras, "A measurement of the light yield of common inorganic scintillators," *IEEE Trans. Nucl. Sci.*, vol. NS-35, pp. 105–109, 1988.

[10] L. M. Bollinger and G. E. Thomas, "Measurement of the time dependence of scintillation intensity by a delayed-coincidence method," *Rev. Sci. Instr.*, vol. 32, pp. 1044–1050, 1961.

[11] W. H. Turner, "Photoluminescence of color filter glass," *Appl. Optics*, vol. 12, pp. 480–486, 1973.

[12] A. A. Kaminskii, *Crystalline Lasers: Physical Processes and Operating Schemes.* Boca Raton: CRC Press, Inc., 1996.

[13] W. W. Moses, A. C. West, S. E. Derenzo, et al., "Internet access to data for scintillation compounds," in *Inorganic Scintillators and Their Applications*, P. Dorenbos and C. W. E. v. Eijk, Eds. Delft, The Netherlands: Delft University Press, 1996, pp. 525–527.

[14] P. Schotanus, P. Dorenbos, and V. D. Ryzhikov, "Detection of CdS(Te) and ZnSe(Te) scintillation light with silicon photodiodes," *IEEE Trans. Nucl. Sci.*, vol. NS-39, pp. 546–550, 1992.

[15] A. N. Gruzintsev, "Investigation of complex anisotropic centers of blue and green luminescence of SrS:Ce by the method of the polarized intracentral photoexcitation," *J. Lumin.*, vol. 71, pp. 207–212, 1997.

[16] W. Lehmann and F. M. Ryan, "Fast cathodoluminescent calcium sulfide phosphors," *J. Electrochem. Soc.*, vol. 119, pp. 275–277, 1972.

[17] J. C. van't Spijker, P. Dorenbos, C. P. Allier, et al., "Lu_2S_3:Ce^{3+}: a new red luminescing scintillator," Delft University of Technology Preprint IRI-ISO-970008, 1997.

[18] S. Yokana, T. Abe, and T. Hoshina, "Red luminescence of Ce^{3+} due to large Stokes shifts in Y_2O_2S and Lu_2O_2S," *J. Lumin.*, vol. 72-4, pp. 171–173, 1997.

[19] T. Danger, K. Petermann, N. Schwentner, et al., "UV-spectroscopy and band structure of Ti:$YAlO_3$," *J. Lumin.*, vol. 24/25, pp. 309–312, 1981.

[20] Z. Bryknar, P. Peka, Z. Potucek, et al., "Infra-red luminescence of mercurous chloride crystals," *Opt. Mater.*, vol. 6, pp. 161–169, 1996.

Table 1. Known rare earth solid state laser transitions.

Wave-length (μm)	Ion	Transition	Comments
0.54	Pr^{3+}	$^3P_0 \rightarrow {}^3H_5$	~100s ms lifetime
0.54	Tb^{3+}	$^5D_4 \rightarrow {}^7F_5$	Well-known, ms lifetime
0.55	Er^{3+}	$^4S_{3/2} \rightarrow {}^4I_{15/2}$	Intense, ~100s ms lifetime
0.55	Ho^{3+}	$^5S_2 \rightarrow {}^5I_8$	Intense, ~100s ms lifetime
0.56	Er^{3+}	$^2H_{9/2} \rightarrow {}^4I_{13/2}$	
0.59	Sm^{3+}	$^4G_{5/2} \rightarrow {}^6H_{7/2}$	Intense, ~0.1-1 ms lifetime
0.60	Pr^{3+}	$^3P_0 \rightarrow {}^3H_6$	
0.61	Eu^{3+}	$^5D_0 \rightarrow {}^7F_2$	Well-known, ms lifetime
0.62	Er^{3+}	$^4G_{11/2} \rightarrow {}^4I_{11/2}$	Luminescence in some hosts
0.62	Er^{3+}	$^2P_{3/2} \rightarrow {}^4F_{9/2}$	Luminescence in some hosts
0.63	Pr^{3+}	$^3P_2 \rightarrow {}^3F_4$	Luminescence in some hosts
0.64	Pr^{3+}	$^3P_0 \rightarrow {}^3F_2$	
0.65	Sm^{3+}	$^4G_{5/2} \rightarrow {}^6H_{7/2}$	Intense, ~0.1-1 ms lifetime
0.65	Tm^{3+}	$^1G_4 \rightarrow {}^3F_4$	
0.67	Er^{3+}	$^4F_{9/2} \rightarrow {}^4I_{15/2}$	Luminescence in some hosts
0.70	Pr^{3+}	$^3P_0 \rightarrow {}^3F_3$	~100s ms lifetime
0.70	Er^{3+}	$^2H_{9/2} \rightarrow {}^4I_{11/2}$	Luminescence in some hosts
0.70	Sm^{2+}	5d, $^5D_0 \rightarrow {}^7F_1$	Intense , lifetime variable
0.72	Pr^{3+}	$^3P_0 \rightarrow {}^3F_4$	~100s ms lifetime
0.73	Nd^{3+}	$^2P_{3/2} \rightarrow {}^4F_{5/2}$	Luminescence in some hosts
0.75	Ho^{3+}	$^5S_2 \rightarrow {}^5I_7$	Intense, 100s ms lifetime
0.80	Tm^{3+}	$^3H_4 \rightarrow {}^3H_6$	
0.80	Tm^{3+}	$^1G_4 \rightarrow {}^3H_5$	
0.85	Er^{3+}	$^4S_{3/2} \rightarrow {}^4I_{13/2}$	Intense, ~100s ms lifetime
0.88	Pr^{3+}	$^3P_1 \rightarrow {}^1G_4$	Luminescence in some hosts
0.91	Pr^{3+}	$^3P_0 \rightarrow {}^1G_4$	~100s ms lifetime
0.93	Nd^{3+}	$^4F_{3/2} \rightarrow {}^4I_{9/2}$	Intense, ~100s ms lifetime
0.93	Pm^{3+}	$^5F_1 \rightarrow {}^5I_5$	Radioactive ion
0.98	Ho^{3+}	$^5F_5 \rightarrow {}^5I_7$	Luminescence in some hosts
0.99	Er^{3+}	$^4I_{11/2} \rightarrow {}^4I_{15/2}$	Intense in some fluorides
0.99	Pr^{3+}	$^1D_2 \rightarrow {}^3F_4$	
1.01	Ho^{3+}	$^5S_2 \rightarrow {}^5I_6$	Intense, ~100s ms lifetime
1.03	Yb^{3+}	$^2F_{5/2} \rightarrow {}^2F_{7/2}$	Intense, long (ms) lifetime
1.04	Pr^{3+}	$^1G_4 \rightarrow {}^3H_4$	Luminescence in some hosts
1.05	Pr^{3+}	$^1D_2 \rightarrow {}^3F_3$	
1.06	Nd^{3+}	$^4F_{3/2} \rightarrow {}^4I_{11/2}$	Intense, ~100s ms lifetime

Table 2. Long Wavelength Luminosities. The measured luminous intensity (in photons per MeV) of the 600–900 nm emissions. Samples marked with an asterisk (*) consist of small (0.5 mm typical dimension) crystals and thus have less optical attenuation than powdered samples, yielding artificially high estimates (typical factor 2–5) for the luminosity.

Photon / MeV	Compound	Phot. /MeV	Compound
123171*	$LuPO_4$:20% Eu	2690	CsI
103244*	$LuPO_4$:30% Eu	2571*	YPO_4:5% Nd
76099*	$LuPO_4$:~5% Eu	2497	Eu_2O_3
61072*	$ScPO_4$:~1% Eu	2468*	$LuPO_4$:0.7% Fe
60316*	$LuPO_4$:5%Eu, 1%Gd	2427	EuF_3
44302*	$ScPO_4$:10% Sm	2418*	$BaLuYF_8$:0.2% Pr
35728	YVO_4:Eu	2401*	$Na_{0.4}Lu_{0.6}F_2$: 1% Nd
31543*	$ScPO_4$:3% Sm	2296	$Bi_2Al_4O_9$: 0.5% Ce
31294*	YPO_4:2% Sm	2271*	$ScPO_4$:2% Dy
22095*	YPO_4:?% Eu	2232	$CaMoO_4$
15728*	$LuPO_4$:2% Sm	2201	LaF_3:1% Pr, 1% Ba
14589*	$ScPO_4$:~5% Eu	2157	Y_2O_3:2% Tb
14288*	$LuPO_4$:10 % Sm	2089*	$ScPO_4$:1.7% Ni
13067	$GdTaO_4$:Tb	1806*	BaF_2:8.4% Ho
13053*	$ScPO_4$:2.9% Dy	1799	LaF_3:0.5% Pr
12101*	YPO_4:1% Dy	1743*	$PbHPO_4$:5.8% Tb
10914*	$ScPO_4$:0.7% Er	1651*	$ScPO_4$:0.7% Fe
10304	BaF_2:10% Eu	1609*	$TbPO_4$:25% Gd
9316*	$LuPO_4$:10% Tb	1526	Y_2O_3:2% Tb, 2% Eu
9280*	$ScPO_4$:10% Pr	1514	TbF_3
9242*	YPO_4:2% Tm	1514	$Lu_3Al_5O_{12}$:Ce
7886	Hg_2Cl_2	1506*	$LaPO_4$:?% Eu
7824*	LaF_3:0.5% Pr	1444*	$LuPO_4$:2% Tm
7658*	$ScPO_4$:2.6% Pr	1427	CdF_2:1% Er
7057*	ZnS:Ag	1425	LaF_3:1% Pr
6748*	$ScPO_4$:1.7% Nd	1389	Al_2O_3
6539	$LuTaO_4$:Tb	1378	$TbCl_3$
5284*	$ScPO_4$:0.7% V	1304	ZnO:0.3 % Al
4776	BaF_2:5% Eu	1288	$3(Zn(OH)_2)•2(ZnCO_3)$
4449*	$ScPO_4$:1% Tb	1137	$SnSO_4$
4399	TiO_2	1133*	BaF_2:10% Er
4293*	$BaNb_2O_6 \cdot SrNb_2O_6$	1128	BaF_2:3% Gd
4143*	$LuPO_4$:0.63% Dy	1088	$LuAlO_3$: 1.5% Ce
4029*	CdS	1079*	$LuPO_4$:3.1% Nd
3856	$Bi_2Al_4O_9$	1073*	SbI_3
3786	SrI_2	1069	BaF_2:1% Eu
3446*	$ScPO_4$:2% Nd	1054	$ThCl_4$
3388*	$Y_{0.5}Gd_{0.5}PO_4$	1040	$Eu_2(CO_3)_3 \cdot x(H_2O)$
3216*	ZnO	1025*	ZnO: 0.6% In
3211*	$SrTiO_3$	1017	$LuAlO_3$: 0.5% Ce
3202	BaF_2:6%Gd, 0.5%Pr	1011	$Bi_4Ge_3O_{12}$
3190*	$ScPO_4$:1.7% Yb	1009	GdF_3:15% Ca, <1%Pr
3110*	BaF_2:6%Gd, 0.2%Pr	994	CdF_2:10% Tb
3060*	YPO_4:0.5% Fe	960	ZrO_2
3036	Hg_2Br_2	959	GdF_3:17% Sr, <1% Pr
3013*	YPO_4:1% Tb	952*	YPO_4:25% Pr
2942*	$Na_{0.4}Y_{0.6}F_2$: 1% Nd	939*	$LuPO_4$:40% Pr
2825*	$LuPO_4$:0.26% Dy	933*	$LuPO_4$:25% Pr
2823*	BaF_2:3% Gd,0.2% Pr	932	ErF_3
2713*	BaF_2:2% Gd,0.2% Pr	930	TbF_3:0.5% Ce

IEEE Trans. Nucl Sci., vol. NS-45, pp. 462–466, 1998